Plastic analysis of reinforced concrete beams

Plastic Analysis of Reinforced Concrete Beams

Analyse plastique des poutres en béton armé

Plastische Berechnung von Stahlbeton-Trägern

BRUNO THÜRLIMANN
Professor of Structural Engineering
Swiss Federal Institute of Technology
Zurich, Switzerland

SUMMARY

Plastic solutions for the strength of reinforced concrete beams under bending, shear, torsion and combined actions are presented. Associated problems of structural details are mentioned. Observations on a relevant comparison of theoretical values with experimental results are made. The practical use in specifications is indicated.

RESUME

Des solutions plastiques sont présentées pour déterminer la résistance ultime des poutres en béton armé soumises à la flexion, à l'effort tranchant, à la torsion et à des efforts combinés. Les détails constructifs correspondants sont également traités. La comparaison des valeurs théoriques avec les résultats expérimentaux donne lieu à quelques remarques. Une application pratique pour des normes est mentionnée.

ZUSAMMENFASSUNG

Plastische Lösungen für den Widerstand von Stahlbetonbalken unter Biegung, Schub, Torsion und kombinierter Beanspruchung werden dargestellt. Auf die entsprechenden konstruktiven Detailprobleme wird hingewiesen. Bemerkungen zu einem sinnvollen Vergleich von theoretischen Werten mit experimentellen Resultaten werden gemacht. Die praktische Anwendung in Normen wird erwähnt.

1. INTRODUCTION

The bending strength of reinforced concrete beams and slabs is determined by assuming a fully plastified stress distribution over the depth of the section. If the steel starts yielding considerably before crushing of the concrete (under reinforced sections), large plastic rotations will occur. Hence, the notions of "plastic hinge" (beams) and "yield line" (slabs) were introduced. The theory of plasticity can then be applied to calculate the collapse load of beams (one-dimensional) or slabs (two-dimensional).

However, the practical calculation of the strength of members subjected to torsion, shear and combined action is still based on rather crude semi-empirical formulas derived from test data.

This report gives a summary of results obtained during the past 10 to 15 years on the application of the theory of plasticity to such cases. In general, the three-dimensional extent of a beam must be taken into account making the analysis accordingly more complicated. Pertinent references are indicated and listed at the end.

2. SHEAR WEB

Beams with rectangular, box-, T-, H- or [-sections can be decomposed into their functional elements, namely flanges or corner stringers subjected to tension or compression and connecting web elements under pure shear. The strength of such a web element will hence be analyzed first ([1], [2], [3], [4]).

A web element subjected to a shear flow, $S = \tau d$, with an orthogonal reinforcement A_x, A_y is shown in Fig. 1. According to the plastic theory the following assumptions are made (Fig. 2):

1. Rigid-plastic material behaviour
2. Forces in the reinforcements only in axial direction, i.e. no shear resistance of the reinforcing net, no doweling action; yield values per unit with p_x, p_y.
3. Zero tensile strength for the concrete; square yield criterion with orthogonality of the plastic strain rates $\dot{\varepsilon}_1$, $\dot{\varepsilon}_2$ with the yield surface.

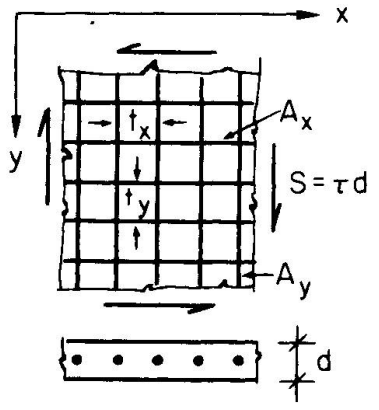

$$a_x = \frac{A_x}{t_y}\,; \qquad a_y = \frac{A_y}{t_x}\,;$$

$$p_x = a_x f_{sx} \qquad p_y = a_y f_{sx}$$

Fig. 1 Shear Web Element

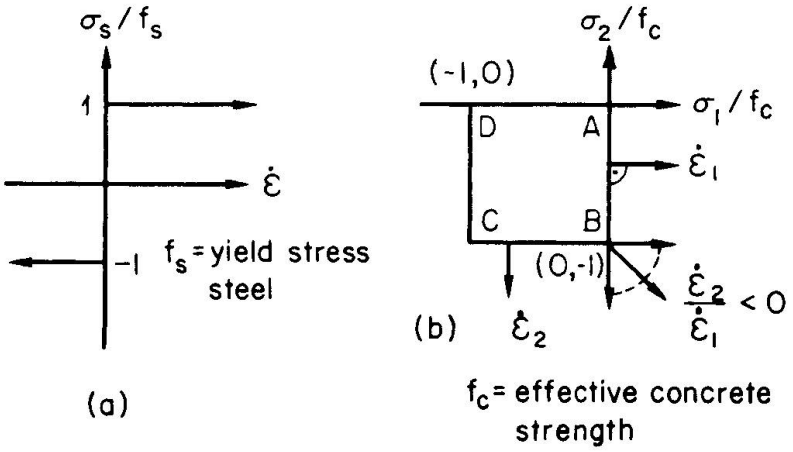

Fig. 2 Yield Criteria

Obviously all deformations up to the onset of unrestricted plastic flow are neglected. Especially previously formed cracks must have a sufficient aggregate interlock to transmit any forces necessary for a redistribution of the concrete stresses. The implication of these assumptions need to be discussed subsequently.

First, an admissible stress field is shown in Fig. 3. The concrete forms a diagonal compression field, $\sigma_1 = 0$, $\sigma_2 = \sigma_c$ under an angle α. The equality between the action $S = \tau d$ and the reactions requires

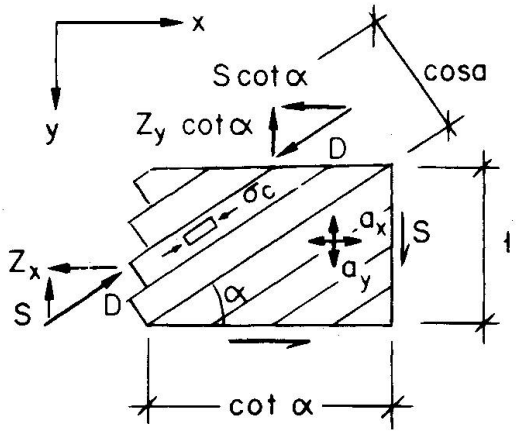

Fig. 3 Admissible Stress Field

$$D = -\sigma_c \cdot d \cdot \cos\alpha \qquad (1)$$

$$Z_x = D \cdot \cos\alpha = S \cdot \cot\alpha \qquad (2)$$

$$Z_y = S \cdot \tan\alpha \qquad (3)$$

Excluding first crushing of the concrete, hence $\sigma_c > -f_c$, the maximum value of the shear flow S_p is reached if both reinforcements yield

$$Z_x = p_x = S_p \cdot \cot\alpha$$

$$Z_y = p_y = S_p \cdot \tan\alpha \quad .$$

Solving for the two unknowns α and S_p gives

$$\tan^2\alpha = \frac{p_y}{p_x} = \lambda \qquad (4)$$

$$S_p = \sqrt{p_x \cdot p_y} = p_y\sqrt{\frac{1}{\lambda}} \qquad (5)$$

$$\sigma_c = -\frac{S_p}{d \cdot \sin\alpha \cdot \cos\alpha} = -\frac{p_y}{d}\left(1 + \frac{1}{\lambda}\right) \qquad (6)$$

$$\lambda = \frac{p_y}{p_x} \quad \text{(ratio of the yield forces)} \qquad (7)$$

For a fixed yield value p_y the yield force p_x can be increased till the strength

of the concrete is reached

$$-\sigma_c = f_c = \frac{p_y}{d}(1+\frac{1}{\lambda})$$

or

$$\lambda_c = \frac{p_y/f_c \cdot d}{1-p_y/f_c \cdot d} \tag{8}$$

Substituting into Eq. (5) gives the shear flow S_{pc} producing concrete failure

$$\frac{S_{pc}}{f_c \cdot d} = \sqrt{\frac{p_y}{f_c \cdot d}(1-\frac{p_y}{f_c \cdot d})} \tag{9}$$

The corresponding required yield force p_{xc} is

$$\frac{p_{xc}}{f_c \cdot d} = \frac{p_y}{f_c \cdot d}\cdot\frac{1}{\lambda_c} = 1-\frac{p_y}{f_c \cdot d} \tag{10}$$

Eqs. (9) and (10) are plotted in Fig. 4(a). Obviously, $p_x = p_y = 1/2 \cdot f_c \cdot d$ gives the maximum possible shear resistance with the inclination $\tan\alpha = 1$ of the concrete compression field. Keeping the total amount of reinforcement constant, $p_x + p_y = f_c \cdot d$, a distribution ratio $\lambda = p_y/p_x$ not equal to unity will diminish the shear resistance. For $p_y \to 0$ and $p_x \to 0$, the inclination reaches $\alpha = 0$ and $\pi/2$, respectively.

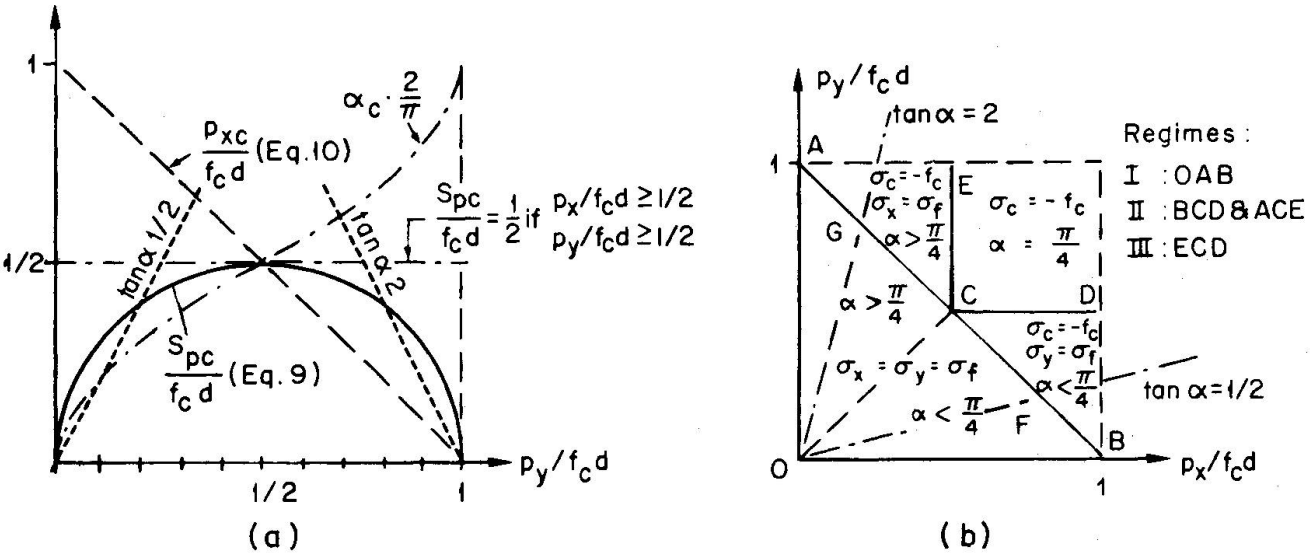

Fig. 4 Collapse Loads and Corresponding Regimes

An actual shear web will first crack at $\pi/4$. A redistribution of the concrete stresses such that extreme values α at collapse occur seems very unlikely. Hence, limiting values, $1/2 < \tan\alpha < 2$, have been proposed to exclude these extremes ([5], [6], [7]). The corresponding restriction is also shown in Fig. 4(a). A considerable reduction of the maximum concrete stresses for low values of $p_y/f_c \cdot d < 0.2$ (or $p_x/f_c \cdot d < 0.2$) are the desired consequence.

The corresponding kinematic solution is considered next. However, a discussion of kinematically admissible velocity fields is needed. In a band of thickness b,

Fig. 5, a linearly varying velocity field is assumed. With $\dot{w}_B$ the displacement rate from B to B' the values are

$$\dot{w} = \frac{\dot{w}_B}{b} \cdot n \tag{11}$$

$$\dot{w}_n = \frac{\dot{w}_B}{b} \cdot n \cdot \cos\vartheta \tag{12}$$

$$\dot{w}_t = \frac{\dot{w}_B}{b} \cdot n \cdot \sin\vartheta \tag{13}$$

and the strain rates

$$\dot{\varepsilon}_n = \frac{\partial \dot{w}_n}{\partial n} = \frac{\dot{w}_B}{b} \cdot \cos\vartheta \tag{14}$$

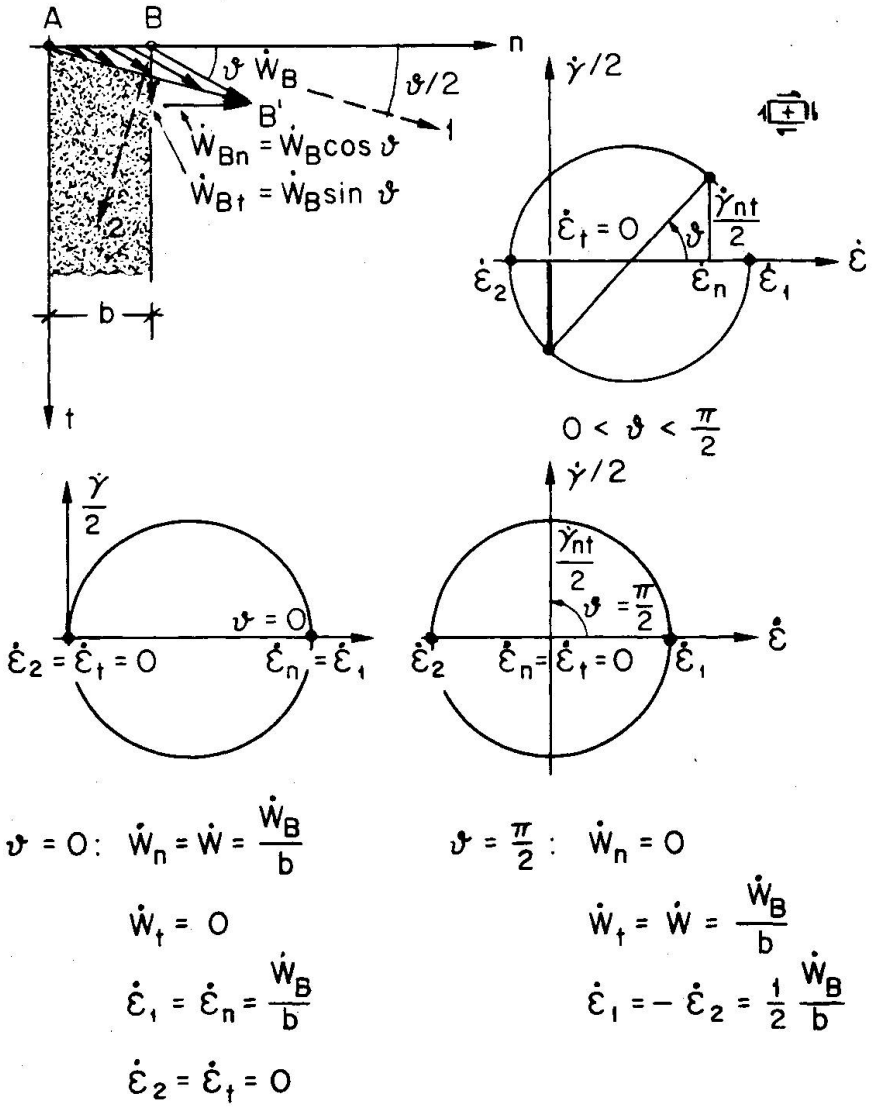

$\vartheta = 0$: $\dot{W}_n = \dot{W} = \frac{\dot{W}_B}{b}$

$\dot{W}_t = 0$

$\dot{\varepsilon}_1 = \dot{\varepsilon}_n = \frac{\dot{W}_B}{b}$

$\dot{\varepsilon}_2 = \dot{\varepsilon}_t = 0$

$\vartheta = \frac{\pi}{2}$: $\dot{W}_n = 0$

$\dot{W}_t = \dot{W} = \frac{\dot{W}_B}{b}$

$\dot{\varepsilon}_1 = -\dot{\varepsilon}_2 = \frac{1}{2}\frac{\dot{W}_B}{b}$

Fig. 5 Kinematics of Slip Bands

$$\dot{\varepsilon}_t = \frac{\partial \dot{w}_t}{\partial t} = 0 \tag{15}$$

$$\dot{\gamma}_{nt} = \frac{\partial \dot{w}_n}{\partial t} + \frac{\partial \dot{w}_t}{\partial n} = \frac{\dot{w}_B}{b} \sin\vartheta \tag{16}$$

Such a field is kinematically admissible as continuity over the band width b is provided. In particular, the strain $\dot{\varepsilon}_t = 0$.

The principal strain directions are indicated in a Mohr's circle, Fig. 5(b):

$$\dot{\varepsilon}_{1,2} = \frac{1}{2}(\dot{\varepsilon}_n + \dot{\varepsilon}_t) \pm \frac{1}{2}\sqrt{(\dot{\varepsilon}_n - \dot{\varepsilon}_t)^2 + \dot{\gamma}_{nt}^2} \tag{17}$$

$$\dot{\varepsilon}_1 = \frac{\dot{w}_B}{2 \cdot b}(1 + \cos\vartheta) \tag{18}$$

$$\dot{\varepsilon}_2 = \frac{\dot{w}_B}{2 \cdot b}(-1 + \cos\vartheta) \tag{19}$$

$$\tan\vartheta = \frac{\dot{\varepsilon}_n - \dot{\varepsilon}_t}{\dot{\gamma}_{nt}} = \frac{\dot{\gamma}_{nt}}{\dot{\varepsilon}_n} \tag{20}$$

The principal direction 1 forms an angle $\vartheta/2$ with the n-axis, hence, it always bisects the angle ϑ between the displacement rate $\dot{w}_B$ and the n-axis as shown in the figure.

The flow rule for concrete (Fig. 2) will now determine the angle ϑ at which $\dot{w}_B$ becomes possible.

Case A-B:

A stress point ($\sigma_1 = 0$; $0 < \sigma_2 < -f_c$) on A-B requires a strain rate $\dot{\varepsilon}_1 > 0$ and $\dot{\varepsilon}_2 = 0$. From Eq. (19) the condition is

$\cos\vartheta = 1 \rightarrow \vartheta = 0$

$\dot{w} = \dot{w}_n$

$\dot{w}_t = 0$

Consequently, the crack band opens perpendicularly to the direction of the compression field. No energy is dissipated in the concrete along the crack

Case B:

A singularity exists at stress point B ($\sigma_1 = 0$; $\sigma_2 = -f_c$). The situation is indeterminate as combinations $\dot{\varepsilon}_2/\dot{\varepsilon}_1 < 0$ become possible. The corresponding situation is described in Fig. 5 with the two extreme cases $\vartheta = 0$ and $\vartheta = \pi/2$. Any situation in between is possible. This behaviour will be of interest when discussing cases, where the concrete stress reaches its strength value f_c.

The basis is now prepared to discuss the kinematic solution for the web element of Fig. 6. The two parts separate normally at the rate $\dot{w}_B$. Equating the internal and external work rates leads to

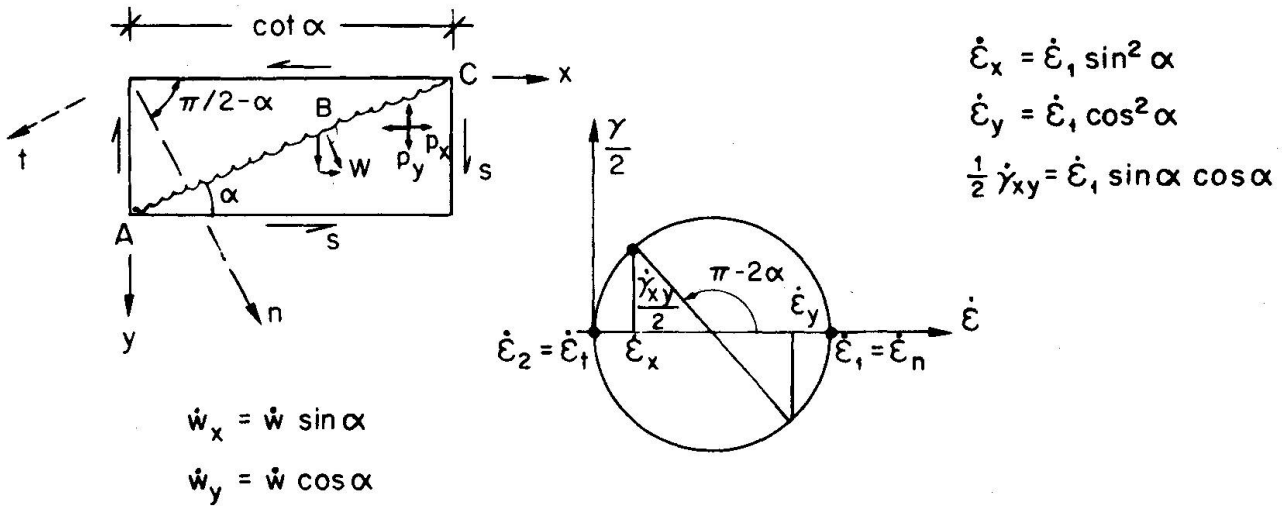

Fig. 6 Admissible Velocity Field

$$L_{in} = p_x \cdot \dot{w}_x + p_y \cdot \cot\alpha \cdot \dot{w}_y = L_{ex} = S \cdot \cot\alpha \cdot \dot{w}_x + S \cdot \dot{w}_y$$

Introducing the $\dot{w}$-values from Fig. 6

$$\dot{w}_x = \dot{w} \cdot \sin\alpha \,, \qquad \dot{w}_y = \dot{w} \cdot \cos\alpha \,, \qquad S = \frac{1}{2}(p_x \cdot \tan\alpha + p_y \cdot \cot\alpha) \,,$$

with the minimum value

$$\frac{\partial S}{\partial \alpha} = 0 = p_x \cdot \frac{1}{\cos^2\alpha} - p_y \cdot \frac{1}{\sin^2\alpha}$$

$$\tan^2\alpha = \frac{p_y}{p_x} = \lambda \qquad (21)$$

$$S_p = \sqrt{p_x \cdot p_y} = p_y \cdot \sqrt{\frac{1}{\lambda}} \qquad (22)$$

The solution coincides with the lower bound solutions Eq. (5). It should be noted that this kinematic solution does not give any information on the concrete stress σ_c.

The strain rates $\dot{\varepsilon}_x$, $\dot{\varepsilon}_y$ and $\dot{\gamma}_{xy}$ are related to $\dot{\varepsilon}_n = \dot{\varepsilon}_1$ as shown in Fig. 6

$$\dot{\varepsilon}_x = \dot{\varepsilon}_n \cdot \sin^2\alpha \,, \qquad \dot{\varepsilon}_y = \dot{\varepsilon}_n \cdot \cos^2\alpha \,, \qquad \dot{\gamma}_{xy}/2 = \dot{\varepsilon}_n \cdot \sin\alpha \cdot \cos\alpha \,.$$

In an actual shear web collapse will occur after considerable elastic and inelastic deformations have taken place. The above strain rate relations at collapse may, however, serve to estimate the total strains. Assuming

$$\frac{\varepsilon_{y\,tot}}{\varepsilon_{x\,tot}} \approx \frac{\dot{\varepsilon}_y}{\dot{\varepsilon}_x} = \cot^2\alpha \qquad (23)$$

$$\frac{\varepsilon_{n\,tot}}{\varepsilon_{x\,tot}} = \frac{\dot{\varepsilon}_y}{\dot{\varepsilon}_x} \approx \frac{1}{\sin^2\alpha} \qquad (24)$$

it follows that for small angles α, i.e. $p_y \to 0$, the $\varepsilon_{x\,tot}$ and $\varepsilon_{n\,tot}$ increase very rapidly. Even a small strain $\varepsilon_{x\,tot}$ below the yield strain of the longitudinal x-reinforcement will cause very large strains in the stirrup y-reinforcement and large cracks, $\varepsilon_{n\,tot}$ representing a "mean crack strain". Again, a limitation on the tolerable value of $\tan\alpha$ seems indicated in order to maintain the aggregate interlock across the cracks.

As previously discussed a mechanism in the form of a slip band will occur if strain rates $\dot{\varepsilon}_2 < 0$ become possible, hence, the concrete stress has reached its strength value $\sigma_c = -f_c$. According to Eqs. (11) and (12)

$$\dot{w}_n = \frac{\dot{w}_B}{n}\cdot\cos\vartheta \quad , \qquad \dot{w}_t = \frac{\dot{w}_B}{n}\cdot\sin\vartheta \quad ,$$

with the corresponding strain rates

$$\dot{\varepsilon}_1 = \frac{\dot{w}_B}{2\cdot b}(1+\cos\vartheta) \quad , \qquad \dot{\varepsilon}_2 = \frac{\dot{w}_B}{2\cdot b}(-1+\cos\vartheta) \quad , \qquad \tan\vartheta = \frac{\dot{\gamma}_{nt}}{\dot{\varepsilon}_n}$$

Referred to the compression field $\sigma_c = -f_c$ with an angle α in the x-, y-system, Fig. 7, the situation is illustrated for three cases. In the range $0 < \alpha < \pi/4$ the x-steel will cease to yield such that $\dot{w}_B = \dot{w}_y$. A slip band (S.B.) will then form under the angle 2α. Energy will now be dissipated by crushing of the concrete. The value of S_p will not change if the yield force p_x is increased over the critical value p_{xc} (Fig. 4(a)) just producing a concrete stress $\sigma_c = -f_c$.

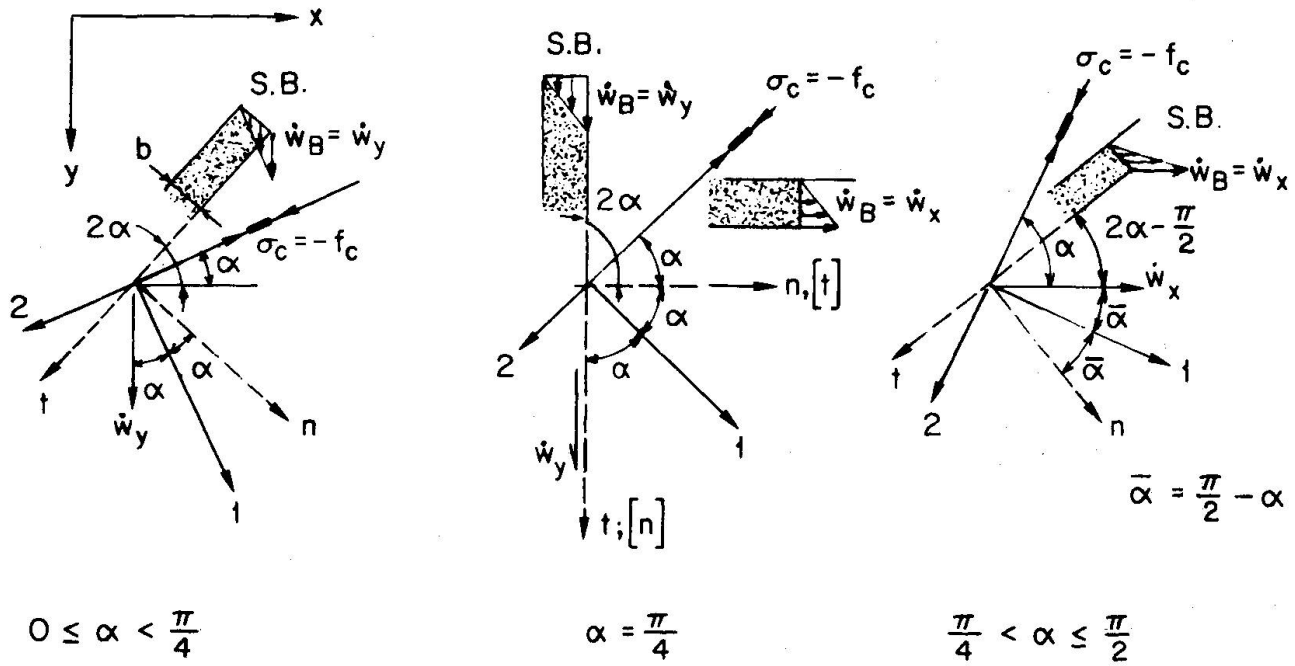

Fig. 7 Orientations of Slip Bands

If $\alpha = \pi/4$ the slip band will reach a vertical (or horizontal) position. Values $\pi/4 < \alpha < \pi/2$ occur if $p_x < p_y$. The slip band turns from the horizontal into the vertical position.

The finding are summirized in Fig. 4(b). Below line AB collapse is governed by yielding of both reinforcements. This yield regime will be termed Regime I. Beyond ECD failure occurs by crushing of the concrete without yielding of the steel (Regime III). In the two triangles AEC and CDB concrete and yielding of one reinforcement are controlling (Regime II). Hence, any increase of p_x in the triangle BDC or any increase of p_y in the triangle AEC will not change the value of S_p. For $p_x/f_c \cdot d = p_y/f_c \cdot d = 1/2$ the maximum possible resistance is reached. The limitations imposed by $1/2 < \tan\alpha < 2$ are cutting off the border regions OBF and OAG, respectively.
In the subsequent sections reference will be made to the three different yield regimes I, II and III defined above.

From a strength point of view the formation of slip bands does not give new information as indicated above. However, the slip mechanisms allow new kinematic configurations if external geometrical restraints are present. Furthermore, they may allow better physical explanations of test observations.

3. TORSION AND BENDING

In a box beam with rectangular cross section $b \cdot h$, Fig. 8, torsion produces a constant shear flow around the perimeter

$$S = \tau d = \frac{T}{2A_o} \qquad (25)$$

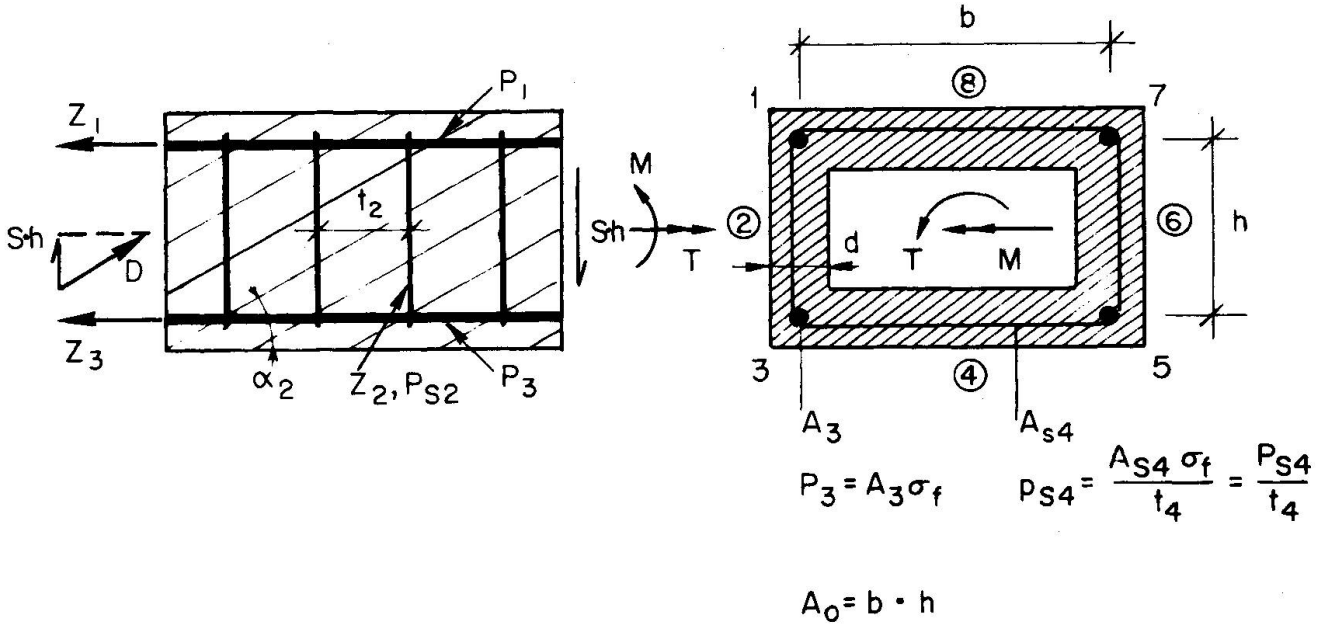

Fig. 8 Box-Section, Space Truss Model

A statical solution is given first. A space truss model is assumed with the stringers as chords, the stirrups as posts and the concrete forming diagonal compression fields under angles α [5], [6]). The walls are under pure shear such that Eqs. (2), (3), (4) and (5) are directly applicable. For wall 2 the following force system develops:

Stirrup force: $Z_2 = S \cdot t_2 \cdot \tan\alpha_2 = p_{s2} \cdot t_2$

Yielding of the stirrups, $Z_2 = p_{s2} \cdot t_2$, fixes the angle α_2:

$$\cot\alpha_2 = \frac{S}{p_{s2}} \tag{26}$$

Horizontal component D_h of compression field:

$$D_{h2} = S \cdot h \cdot \cot\alpha_2 \tag{27}$$

Failure may occur by yielding of the stirrups and the two lower stringers (Regime I). Equilibrium of the internal forces with respect to the axis 1-7 gives

$$D_{h2} \cdot \frac{h}{2} + D_{h4} \cdot h + D_{h6} \cdot \frac{h}{2} - Z_3 \cdot h - Z_5 \cdot h = 0 \tag{28}$$

Replacing Z_3 and Z_5 by the yield forces P_3 and P_5 of the stringers and making use of Eqs. (26) and (27) gives

$$S^2 = \frac{P_3 + P_5}{\frac{h}{2}\left(\frac{1}{p_{s2}} + \frac{1}{p_{s6}}\right) + b \cdot \frac{1}{p_{s4}}} \tag{29}$$

and the collapse moment T_{po}

$$T_{po} = 2A_o \sqrt{\frac{P_3 + P_5}{\frac{h}{2}\left(\frac{1}{p_{s2}} + \frac{1}{p_{s6}}\right) + b\,\frac{1}{p_{s4}}}} \tag{30}$$

For a constant stirrup reinforcement around the perimeter and equal stringers in all corners

$p_s = p_{s2} = p_{s4} = p_{s6}$; $\quad u = 2(h+b)$ (perimeter)

$P = P_1 = P_3 = P_5 = P_7$; $\quad A_o = b \cdot h$ (enclosed area)

the resulting expression is

$$T_{po} = 2A_o \sqrt{\frac{4P \cdot p_s}{u}} \tag{31}$$

The analysis has been extended to beams with polygonal cross sections and arbitrary reinforcements. Physically the compression fields in all walls take inclinations depending on the yield values p_s and the shear flow, Eq. (26). The stringers connecting the two rigid parts across the failure zone have to resist the horizontal components of the compression field in the walls. Failure occurs if all but two stringers in one wall will yield.

If in addition to torsion a bending moment is acting its influence on the stringer

forces have to be taken into account. Assuming for simplicity a section with constant reinforcements:

Upper stringers: $P_1 = P_7 = P_u \leqslant P_l$

Lower stringers: $P_3 = P_5 = P_l$

Stirrups : p_s

A part of the yield forces in the lower stringers will be used up by the bending moment

$$M_p = 2 \cdot h \cdot \eta \cdot P_l \; ; \qquad \eta \leqslant 1$$

Accordingly, the torsional moment will be reduced to

$$T_p = 2A_o \sqrt{\frac{4(1-\eta) \cdot P_l \cdot p_s}{u}}$$

Introducing the reference values

$$M_{po} = 2 \cdot h \cdot P_l$$

$$T_{po} = 2A_o \sqrt{\frac{4P_u \cdot p_s}{u}}$$

where T_{po} is governed by the smaller yield value $P_u < P_l$ (failure about axis 3-5 through lower stringers) the following interaction equations can be derived

Yielding $Z_l = P_l$:
$$\frac{P_u}{P_l}\left(\frac{T_p}{T_{po}}\right)^2 + \frac{M_p}{M_{po}} = 1 \qquad (32)$$

Yielding $Z_u = P_u$:
$$\left(\frac{T_p}{T_{po}}\right)^2 - \frac{P_l}{P_u} \cdot \frac{M_p}{M_{po}} = 1 \qquad (33)$$

Recently, the corresponding kinematic solution has been developed ([8], [9]). In Fig. 9 a kinematically admissible mechanism is presented. Starting from the fact that a crack ABC over two sides is only possible if the shape of the cross-section is distored, a second crack DEF on the two opposite sides is added in order to restore the original shape. In this way a parallelogram CBFE on side 4 is cut out. A rotation $\dot{\omega}$ around the axis AD through the crack ends becomes possible if the axis AD is parallel to the line CF, hence, $l_{AD} = l_{CF}$. For the displacement of point F will be perpendicular to the axis AD. On the other hand, F being located on the parallelogram will rotate perpendicularly to line FC, hence, FC parallel to AD. The angles of the two cracks CB and EF being identical, α_4, the angle β of the axis AD follows to

$$l_{CF} = b \cdot \cot\alpha_4 + h \cdot \cot\alpha_2 - l_{AD} + h \cdot \cot\alpha_6 + b \cdot \cot\alpha_4$$

with: $l_{CF} = l_{AD}$ and $\cot\beta = \frac{l_{AD}}{b}$

$$\cot\beta = \cot\alpha_4 + \frac{1}{2} \cdot \frac{h}{b}(\cot\alpha_2 + \cot\alpha_6) \qquad (34)$$

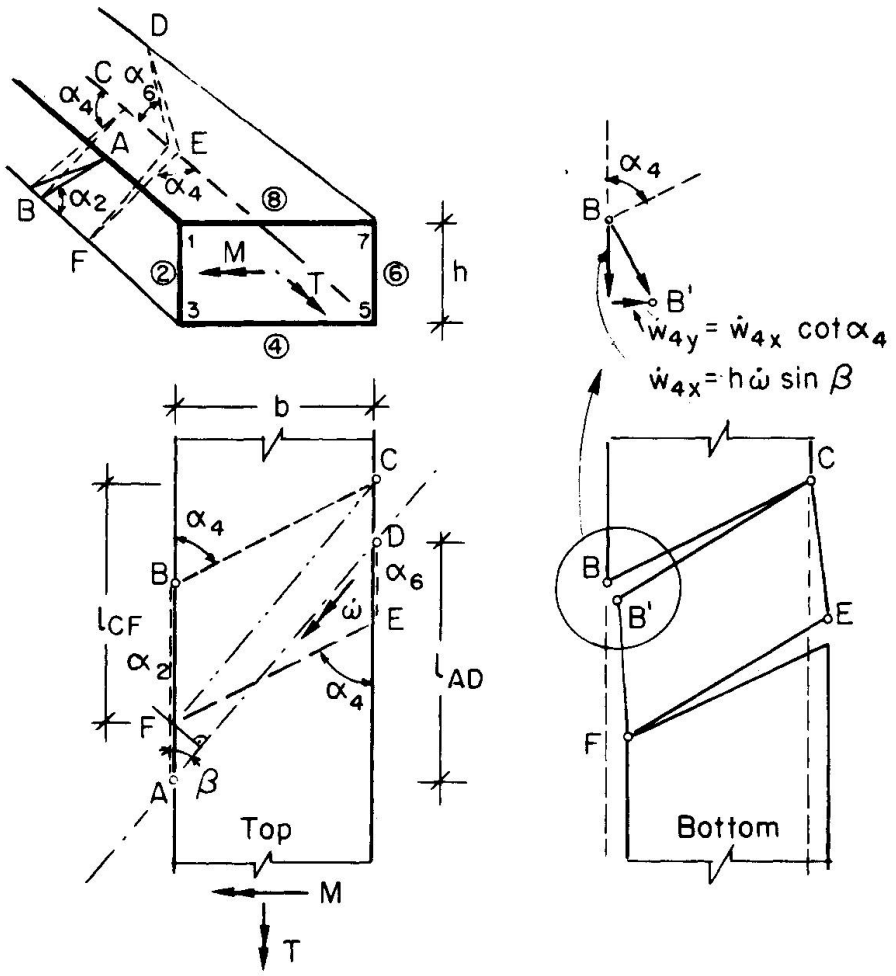

Fig. 9 Torsional Mechanism

It should be remarked that the "skew bending theory" ([10]) uses a mechanism which introduced sliding in a crack. However, the corresponding energy dissipation is erroneously neglected. Hence, the discrepancies with correct plastic solutions can be fully explained.

In order to express the energy dissipation the velocity components of point B (equal to point E) are needed (Fig. 9)

Wall 4: $\dot{w}_{4x} = \dot{\omega} \cdot h \cdot \sin\beta$, $\dot{w}_{4y} = \dot{w}_{4x} \cdot \cot\alpha_4$

Wall 2: $\dot{w}_{2x} = \dot{\omega} \cdot h \cdot \sin\beta$, $\dot{w}_{2y} = \dot{w}_{2x} \cdot \cot\alpha_2$

Using the reinforcements shown in Fig. 8 the work equation takes the form

$$L_{in} = \dot{w}_{4x}(P_3+P_5) + \frac{1}{2} \cdot p_{s2} \cdot h \cdot \dot{w}_{2x} \cdot \cot^2\alpha_2 + p_{s4} \cdot b \cdot \dot{w}_{4x} \cdot \cot^2\alpha_4 + \frac{1}{2} \cdot h \cdot \dot{w}_{6x} \cdot \cot^2\alpha_6 \cdot p_{s6}$$

$$L_{ex} = M \cdot \dot{\omega} \cdot \sin\beta + T \cdot \dot{\omega} \cdot \cos\beta$$

$$M + T \cdot \cot\beta = h(P_3+P_5) + \frac{1}{2} \cdot p_{s2} \cdot h^2 \cdot \cot^2\alpha_2 + p_{s4} \cdot b \cdot h \cdot \cot^2\alpha_4 + \frac{1}{2} \cdot p_{s6} \cdot h^2 \cdot \cot^2\alpha_6$$

Introducing $\cot\beta$ from Eq. (34) gives

$$M = h(P_3+P_5) + \frac{1}{2}(h^2 \cdot p_{s2} \cdot \cot^2\alpha_2 - \frac{h}{b} \cdot T \cdot \cot\alpha_2) + \frac{1}{2}(h^2 \cdot p_{s6} \cdot \cot^2\alpha_6 - \frac{h}{b} \cdot T \cdot \cot\alpha_6) + \frac{b}{h}(h^2 \cdot p_{s4} \cdot \cot^2\alpha_4 - \frac{h}{b} \cdot T \cdot \cot\alpha_4) \quad (35)$$

If T is fixed the minimum value of M with respect to the angles α follows from

$$\frac{\partial M}{\partial(\cot\alpha_2)} = 2 \cdot h^2 \cdot p_{s2} \cdot \cot\alpha_2 - \frac{h}{b} \cdot T = 0$$

$$\cot\alpha_2 = \frac{T}{2 \cdot b \cdot h} \cdot \frac{1}{p_{s2}} = \frac{S}{p_{s2}} \quad ; \qquad S = \frac{T}{2 \cdot b \cdot h} = \frac{T}{2A_o}$$

and similarly: $\cot\alpha_4 = \frac{S}{p_{s4}}$; $\cot\alpha_6 = \frac{S}{p_{s6}}$

Hence, the minimum M will result if T produces a constant shear flow S. This corresponds to the assumption of a constant flow in the statical solution, Eq. (25). In the case of M = 0, Eq. (35) gives the torsional moment T_{po} by introducing the values of $\cot\alpha$:

$$T_{po} = 2A_o \sqrt{\frac{P_3 + P_5}{\frac{h}{2}(\frac{1}{p_{s2}} + \frac{1}{p_{s6}}) + \frac{b}{p_{s4}}}} \quad (36)$$

With a moment M acting, Eq. (35) leads to interaction equations identical to Eqs. (32) and (33). Hence, the identity between the static and kinematic approach has been shown.

The total length of the mechanism is:

$$l_{AC} = h \cdot \cot\alpha_2 + b \cdot \cot\alpha_4 \ , \qquad \text{if } \cot\alpha_2 > \cot\alpha_6$$

or

$$l_{DF} = b \cdot \cot\alpha_4 + h \cdot \cot\alpha_6 \ , \qquad \text{if } \cot\alpha_6 > \cot\alpha_2$$

If geometrical restraints do not allow such a length warping will become necessary and a higher resistance will result. Statical solutions with a constant shear flow hence become lower bounds.

The case may also arise, where the statical solution would imply a concrete stress exceeding the strength $\sigma_c < -f_c$ in a particular wall (Regimes II or III). A redistribution of the stress field will take place leading to a non-uniform shear flow around the perimeter. A safe value is obtained if the solution with constant shear flow but $\sigma_c < -f_c$ is reduced by the factor $-f_c/\sigma_c$.

The above mentioned problems have been treated in Refs. [9] and [11]. The case of beams with open cross sections including warping has also been studied [12].

So far, only box-sections have been considered. However, in Ref. [9] it is shown that the previously discussed mechanisms are kinematically admissible also for solid cross-sections. The beam parts are separating internally in perpendicular directions. The parts are touching only along the perimeter. In reality the concrete stresses have to be transmitted over a finite wall thickness in order to

stay above the value $-f_c$. The determination of the effective wall thickness can only be made on the basis of experimental studies. In Refs. [5] and [6] such values have been proposed.

The secondary effect due to distortion of the side walls of a box section, i.e. plate bending, influences only the concrete stresses as the membrane stresses of the compression field are superimposed by secondary bending stresses ([5], [6]). Again this influence must be taken into account in a pragmatic manner by adopting a cautious value for the effective concrete strength.

4. SHEAR AND BENDING

As a statical model a truss model, Fig. 10, is used with the upper and lower stringers as chords, the stirrups as posts and the concrete as diagonal compression field under an angle α ([5], [7]):

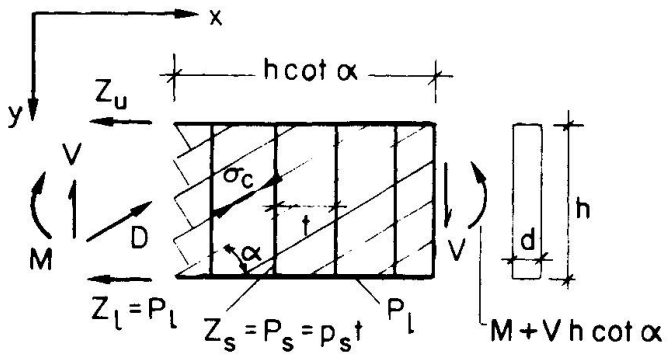

$$D = \frac{V}{\sin\alpha} \tag{37}$$

$$Z_l = \frac{M}{h} + \frac{1}{2}\cdot V\cdot\cot\alpha = P_l \tag{38}$$

$$Z_u = -\frac{M}{h} + \frac{1}{2}\cdot V\cdot\cot\alpha \tag{39}$$

$$Z_s = \frac{V\cdot t}{h}\cdot\tan\alpha = p_s\cdot t \tag{40}$$

$$\sigma_c = \frac{-D}{d\cdot h\cdot\cos\alpha} = -\frac{V}{d\cdot h}\cdot\frac{1}{\sin\alpha\cdot\cos\alpha} \tag{41}$$

Fig. 10 Truss Model Bending - Shear

The stirrup reinforcement is constant along the axis. The lower stringer reinforcement varies such that the yield value $P_l(x)$ is just reached at a critical section, hence, $Z_u = P_l(x)$. Excluding concrete failure the stirrup force Z_s will also reach the yield value $p_s\cdot t$ (Regime I). Replacing in Eq. (38) $\cot\alpha$ by its value from Eq. (40) gives the interaction equation

$$M_p + \frac{V_p^2}{2p_s} = P_l\cdot h$$

With the reference values

$$M_{po} = P_l\cdot h \quad ; \qquad V_{po} = \sqrt{2P_l\cdot p_s\cdot h}$$

$$\frac{M_p}{M_{po}} + \left(\frac{V_p}{V_{po}}\right)^2 = 1 \tag{42}$$

However, a limiting value is reached when $\sigma_c = -f_c$ (Regime II):

$$\sigma_c = -\frac{V}{d\cdot h}\cdot\frac{1}{\sin\alpha\cdot\cos\alpha} = -f_c$$

$$V_{pc} = p_{sc}\cdot h\cdot\cot\alpha$$

Hence, $$\frac{p_{sc}}{f_c\cdot d} = \sin^2\alpha$$

and

$$\frac{V_{pc}}{f_c \cdot d \cdot h} = \sqrt{\frac{p_{sc}}{f_c \cdot d}\left(1 - \frac{p_{sc}}{f_c \cdot d}\right)}$$

with the maximum value

$$\frac{\partial V_{pc}}{\partial\left(\frac{p_s}{f_c \cdot d}\right)} = 0 \quad ; \quad \frac{p_{sc}}{f_c \cdot d} = \frac{1}{2} \; ; \; \left(\frac{V_{pc}}{f_c \cdot d \cdot h}\right)_{max} = \frac{1}{2}$$

Introducing as reference value the maximum value V_{fc} governed by the concrete strength alone (Regime III):

$$V_{fc} = \frac{1}{2} \cdot f_c \cdot d \cdot h \tag{43}$$

the ratio becomes (Fig. 11(b)):

$$\frac{V_{pc}}{V_{fc}} = 2 \sqrt{\frac{p_{sc}}{f_c \cdot d}\left(1 - \frac{p_{sc}}{f_c \cdot d}\right)} \tag{44}$$

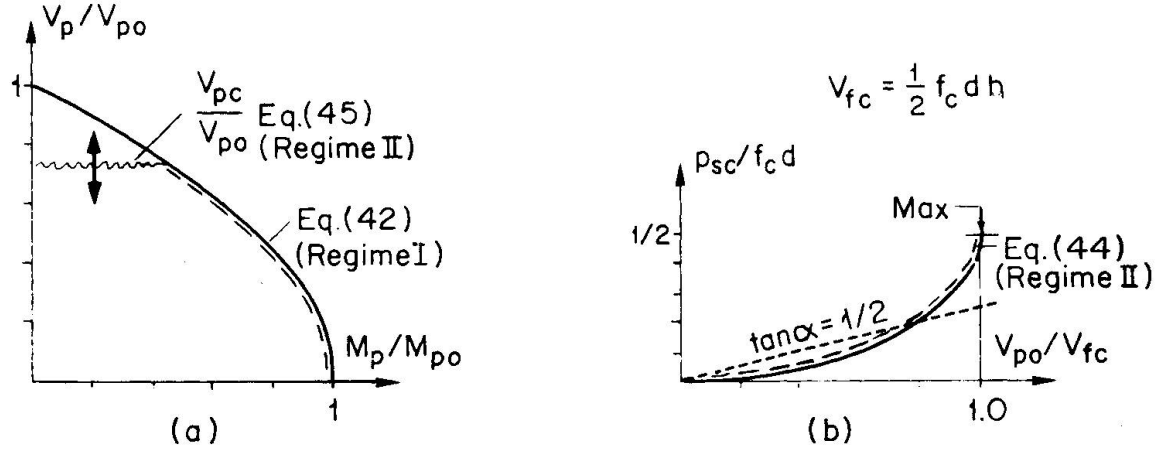

Fig. 11 Interaction Bending - Shear

The interaction Eq. (42) will be cut off if V_p reaches the value V_{pc}, hence,

$$\frac{V_{pc}}{V_{po}} = \sqrt{\frac{V_{fc}}{P_1}\left(1 - \frac{p_{sc}}{f_c \cdot d}\right)} = \sqrt{\frac{V_{fc} \cdot h}{M_{po}}\left(1 - \frac{p_{sc}}{f_c \cdot d}\right)} \tag{45}$$

These relations are shown in Fig. 11(a) and (b). Also indicated is the influence of a limitation $\tan\alpha = 1/2$ for reasons discussed previously.

Turning to the kinematic solution the mechanism is sketched in Fig. 12 ([5], [7], [13], [14]). The work equation gives:

$$M_p \cdot \dot{\omega} + V_p \cdot \dot{\omega} \cdot h \cdot \cot\alpha = P_1 \cdot \dot{\omega} \cdot h + \frac{1}{2} \cdot \dot{\omega} \cdot h \cdot \cot\alpha \cdot p_s \cdot h \cdot \cot\alpha$$

$$M_p = -V_p \cdot h \cdot \cot\alpha + \frac{1}{2} \cdot h^2 \cdot p_s \cdot \cot^2\alpha$$

with the minimum

$$\frac{\partial M_p}{\partial(\cot\alpha)} = -V_p \cdot h + h^2 \cdot p_s \cdot \cot\alpha \rightarrow \cot\alpha = \frac{V_p}{h \cdot p_s}$$

Using the previously introduced reference values M_{po} and V_{po} the interaction Eq. (42) is again obtained. Hence, the two solutions are identical.

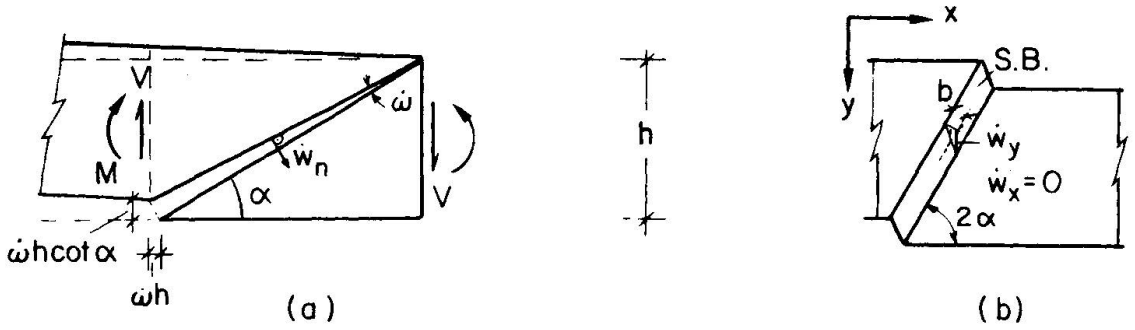

Fig. 12 Mechanism Bending - Shear

The mechanism of Fig. 12(b) corresponds to the case, where the lower stringer is not yielding but instead the concrete is failing, i.e. $\dot{\varepsilon}_2 < 0$ (Regime II). As discussed in chapter 2 a slip band (S.B.) will form at an angle 2α with α being the angle of the compression field. The collapse load will be identical to the solution, Fig. 12(a) for such a value of P_1 that $\sigma_c = -f_c$ will just be reached (transition Regime I to Regime II).

Concerning the strain ratios the same remarks hold as made under chapter 2, Eqs. (23) and (24). A small longitudinal strain $\varepsilon_{x\ tot}$ will produce very large stirrup strains $\varepsilon_{y\ tot}$ and crack strains $\varepsilon_{n\ tot}$ and a progressive break-down of the aggregate interlock for small angles α. Hence, again the necessity for a limitation of $\tan\alpha \geq 1/2$ is evident.

For a general case, where bending M, shear V and torsion T are acting on a box beam such as shown in Fig. 8, statical solutions have been presented assuming a constant shear flow for torsion superimposed by shear forces V/2 in the two side walls [5]. Interaction equations can readily be developed. Corresonding kinematic solutions have not been found. It has, however, been shown for special cases that warping effects will take place [9], [11]. Hence, the statical solution described above constitutes only a lower bound.

So far, all solutions presented have taken into account the spacial dimensions of the beams also in the transverse directions. However, beam theories for closed and open cross-sections have already been developed paralleling in concept the one-dimensional elastic beam theory ([9], [12]). Introducing as generalized stresses the resultants N, M, V and T the corresponding kinematic terms (generalized strains) in the form of extension-, curvature-, shearing- and warping-rates along the beam axis have to be properly selected. The yield criterion and the flow rules are then expressed as functions of these generalized stresses and strains. For cases when collapse is governd solely by yielding of the reinforcements (Regime I) complete beam theories have been worked out. Difficulties arise when strain rates $\dot{\varepsilon}_2 < 0$ for the case $\sigma_c = -f_c$ (point B, Fig. 2(b), (Regime II))

arise. At present, it seems improbably that for such cases a general beam theory can be developed.

5. DETAILS

Problems of structural details and some special problems are shortly indicated and appropriate references are given.

The case of concentrated loads or reactions is sketched in Fig. 13. The length $h \cdot \cot\alpha$ of the regular compression field is concentrated by a compression fan into the width e resulting into a uniform distribution of P over e. It can be easily shown by geometric relations that the concrete stress σ_c of the regular field increases at point A to σ_{cA}

$$\sigma_{cA} = \sigma_c \cdot \frac{h}{e} \cdot \cot\alpha$$

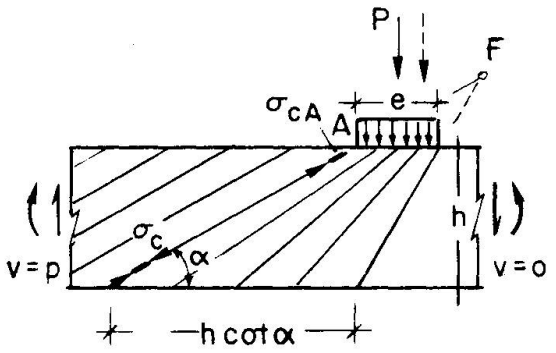

Fig. 13 Compression Fan under Concentrated Load

Hence, a relatively high stress concentration may occur. With a multi-centered fan resulting into a shift of the load P to the right and hence a non-uniform bearing stress more favourable conditions are obtained. Nevertheless, the problem of stress concentrations in such cases has to be taken into account. Further cases of end and intermediate reactions, indirect load applications through cross beams, etc. are studied in Refs [5], [9].

The proportioning of the longitudinal steel in the tension flange of a beam is essentially governed by Eq. (38). The problem of the anchorage length of bars beyond the theoretical cut off point is presented in Ref. [5].

Joints connecting beams and columns have been plastically analyzed (references mentioned in [14]). They offer special problems as transverse splitting of the elements is a distinct failure possibility.

In Ref. [9] the influences of a variable beam depth, of distributed loads and single concentrated loads are studied and the consequences for the detailing of the stirrup and longitudinal reinforcement are stated.

The membrane stress state produced by shear in a shear web can be disturbed by transverse bending moments. A box girder bridge presents such a case, where the side walls are subjected to shear in longitudinal direction and transverse bending moments resulting from transverse bending of the road slab. A static solution [15] and a complete solution [16] have been developed for this case.

6. THEORY, EXPERIMENTAL VERIFICATION, APPLICATION

Plastic solutions for the strength of beams with general cross sectional shapes subjected to bending, shear, torsion and combined actions have been developed. For many cases the correct solutions are known (i.e. static equal to kinematic solution). For other cases lower (static) and/or upper (kinematic) bounds are available.

The necessary structural details (stirrup spacing, stringer arrangement, concentrated loads, bar cut-off, etc.) have or can be developed especially from the statical solutions, where the admissible stress fields furnish the required information.

All these solutions are correct within the assumptions of the theory of plasticity, essentially

1. Rigid-ideally plastic material behaviour
2. Yield criteria and associated flow rules.

Hence, experimental verifications should essentially concentrate on checks of these assumptions and possible adjustments.

Concerning the reinforcing steels they exhibit generally plastic deformations under the yield stress which are a multiple of the elastic deformations such that the latter can be neglected. On the contrary the strength of concrete is definitely affected by deformations and/or cracks preceding failure. A considerable redistribution of the concrete stresses from initial cracking up to collapse (i.e. variation of $\alpha = \pi/4$ to $\alpha \to 0$ or $\alpha \to \pi/2$ of the compression field) accompanied by considerable cracking will markedly diminish the strength. The redistribution may further be limited by the progressive deterioration of the aggregate interlock in previously formed cracks such that the orthogonality required by the flow rules may no longer hold.

The assessment of the effective concrete dimensions offers another problem. Under conditions, where the concrete strength is governing and large redistributions occur the concrete cover may spall off prior to failure. In other instances when failure due to yielding of the reinforcement occurs at low concrete stresses the cover will stay intact.

Only results from experiments on properly detailed specimens (see chapter 5) tested under clearly definited conditions (e.g. necessary extent of mechanism, chapter 3) should be compared with the corresponding theoretical values. It is evident that tests with premature failures of details and/or unclear testing conditions must be excluded.

Considerable experimental evidence has already been collected supporting the applicability of plastic analysis to determine the ultimate strength of reinforced concrete beams. A proper and cautious selection of the effective concrete strength f_c must be made reflecting the above mentioned influences. The fixing of the effective concrete dimensions becomes important if failure is governed by the concrete strength and large redistributions.

It is felt that plastic analysis offers a rational, unified, simple, economical, safe and reasonably accurate method to calculate the static strength of reinforced concrete beams (and slabs and walls as well). It will become more generally applied as the concept of limit state design is gaining general acceptance. For in this concept one of the limit states to consider is the ultimate limit state.

So far design rules for beams under bending, shear, torsion and combined actions based on plastic analysis have already been introduced in the Swiss specifications [19] and the new CEB Model-Code (Shear, Torsion, refined method) ([17], [18], [20]).

References

1 Nielsen, M.P.: "Yield Conditions for Reinforced Concrete Shells in the Membrane State", Reprint from Non-Classical Shell Problems, Proc. IASS Symposium Warsaw, Sept. 2.-5. 1963.

2 Nielsen, M.P.: "On the Strength of Reinforced Concrete Discs", Acta Polytechnica Scandinavica, Copenhagen, 1971, p. 261.

3 Jensen, B.C.: "Lines of Discontinuity for Displacements in the Theory of Plasticity of Plain and Reinforced Concrete", Magazine of Concrete Research, Vol. 27, No. 92, 1975, p. 143.

4 Marti, P., Thürlimann, B.: "Fliessbedingung für Stahlbeton mit Berücksichtigung der Betonzugfestigkeit" (Yield Criteria for Reinforced Concrete Including the Tensile Strength of Concrete), Beton- und Stahlbetonbau, Heft 1, 1977.

5 Thürlimann, B., Grob, J., Lüchinger, P.: "Torsion, Biegung und Schub in Stahlbetonträgern" (Torsion, Bending and Shear in Reinforced Concrete Beams), Institut für Baustatik und Konstruktion, ETH Zürich, Autographie zu Fortbildungskurs für Bauingenieure aus der Praxis, 1975.

6 Lampert, P., Thürlimann, B.: "Ultimate Strength and Design of Reinforced Concrete Beams in Torsion and Bending", Publications, International Association for Bridge and Structural Engineering (IABSE), Vol. 31-I, p. 107, 1971.

7 Grob, J., Thürlimann, B.: "Ultimate Strength and Design of Reinforced Concrete Beams under Bending and Shear", Publications, International Association for Bridge and Structural Engineering (IABSE), Vol. 36-II, p. 105, 1976.

8 Müller, P.: "Failure Mechanisms for Reinforced Concrete Beams in Torsion and Bending", Publications, International Association for Bridge and Structural Engineering (IABSE), Vol. 36-II, p. 147, 1976.

9 Müller, P.: "Plastische Berechnung von Stahlbetonscheiben und -balken" (Plastic Analysis of Walls and Beams of Reinforced Concrete), Institut für Baustatik und Konstruktion, ETH Zürich, Bericht Nr. 83, Birkhäuser Verlag Basel und Stuttgart, 1978.

10 Gvozdev,A.A., Lessig, N.N., Rulle, L.K.: "Research on Reinforced Concrete Beams Under Combined Bending and Torsion in the Soviet Union"; Torsion of Structural Concrete, Journal American Concrete Institute, April 1968, p. 310, Publication SP-18.

11 Lüchinger, P.: "Bruchwiderstand von Kastenträgern aus Stahlbeton unter Torsion, Biegung und Querkraft" (Ultimate Strength of Box-Girders in Reinforced Concrete under Torsion, Bending and Shear), Institut für Baustatik und Konstruktion, ETH Zürich, Bericht Nr. 69, Birkhäuser Verlag Basel und Stuttgart, 1977.

12 Grob, J.: "Traglast von Stäben mit dünnwandigen offenen Querschnitten" (Ultimate Strength of Beams with Thin-Walled Open Cross-Sections), Institut für Baustatik und Konstruktion, ETH Zürich, Bericht Nr. 56, Birkhäuser Verlag Basel und Stuttgart, 1975.

13 Braestrup, M.W.: "Plastic Analysis of Shear in Reinforced Concrete", Magazine of Concrete Research, Vol. 26, No. 89, December 1974.

14 Nielsen, M.P., Braestrup, M.W., Bach, F.: "Rational Analysis of Shear in Reinforced Concrete Beams", Proceedings, IABSE, P-15/78, May 1978.

15 Thürlimann, B.: " Schubbemessung bei Querbiegung" (Shear Design considering Cross Bending), Schweiz. Bauzeitung, Heft 26, p. 478, 1977.

16 Marti, P., Thürlimann, B.: "Shear Strength of Reinforced Concrete Walls with Transverse Bending", (in preparation).

17 Thürlimann, B.: "Shear Strength of Reinforced and Prestressed Concrete Beams - CEB Approach", ACI-Symposium 1976, Philadelphia, (Proceedings in preparation).

18 Thürlimann, B.: "Torsional Strength of Reinforced and Prestressed Concrete Beams - CEB Approach", ACI-Symposium 1976, Philadelphia (Proceedings in preparation).

19 Richtlinie 34 zu Norm SIA 162, 'Bruchwiderstand und Bemessung von Stahlbeton- und Spannbetontragwerken' (Directive RL 34 to Structural Design Code SIA 162 (1968)), Schweizerischer Ingenieur- und Architekten-Verein, Zürich, 1976.

20 Comité Euro-International du Béton: "Code modèle pour les structures en béton", Système international de règlementation technique unifiée des structures, vol. II, Bulletin d'Information, No. 117, Paris, décembre 1976.